Stanford Exploration Project, Report 73, November 18, 1997, pages 325–338

Solving the frequency-dependent eikonal equation

Biondo Biondi[1]

keywords: *phase, modeling, ray tracing, anomaly, amplitudes, velocity*

ABSTRACT

The eikonal equation that is commonly used for modeling wave propagation is frequency independent. Therefore, it cannot correctly model the propagation of seismic waves when rapid variations in the velocity function cause frequency dispersion of the wavefield. I propose a method for solving a frequency-dependent eikonal equation, that can be derived from the scalar wave equation without approximations. The solution of this frequency-dependent eikonal is based on the extrapolation of the phase-slowness function downward along the frequency axis starting from infinite frequency, where the phase slowness is equal to the medium slowness. The phase slowness is extrapolated by solving a non-linear partial differential equation using an explicit integration scheme. The extrapolation equation contains terms that are functions of the phase slowness, and terms that are functions of the ray density. When the terms that are dependent on the rays are neglected, the extrapolation process progressively smooths the slowness model; this smoothing is frequency-dependent and consistent with the wave equation.
Numerical experiments of wave propagation through two simple velocity models show that the solution of the frequency-dependent eikonal computed using the proposed method matches the results of wave-equation modeling significantly better than the solution of the conventional eikonal equation.

INTRODUCTION

When the eikonal equation is solved for modeling wave propagation, the seismic traveltimes are assumed to be frequency independent (Bleistein, 1984; Červený, 1987). This assumption does not always hold for reflection seismic data; its range of validity is limited by the the rate of variation of the wave amplitudes, compared with the frequency of the wavefield (Beydoun, 1985; Woodward, 1990). In particular, when the variations in the velocity function have wavelengths similar to the wavelength of the propagating waves, the traveltimes are not frequency independent and cannot

[1]**email:** not available

be evaluated by simply solving the conventional eikonal equation. Media where this phenomenon happens are called "dispersive", because wave components having different frequencies, or wavelengths, propagate along different "wave-paths", and thus the wavefronts are dispersed (Woodward, 1990). In dispersive media, modeling by solving the conventional eikonal equation not only causes errors in the computed traveltimes, but it also causes errors in the evaluation of the directions of propagation of seismic energy. All frequencies are erroneously assumed to travel along the wave-path corresponding to infinite frequency; that is the "ray paths". Often, in such media, the solution of the eikonal shows some "pathological" behavior such as caustics and shadow zones, while the solution of the full wave equation, with band-limited sources, is well behaved.

On the other hand, the modeling of wave propagation by computing traveltimes with raytracing (Bleistein, 1984; Červený, 1987), or with finite differences, (Vidale, 1988; VanTrier and Symes, 1991), or with traveltime minimization (Moser, 1989) is very attractive because it is far less expensive than solving the full wave equation. Further, there are many applications, for example seismic tomography and Kirchhoff migration, where raytracing is preferred over wave-equation modeling because its results are easier to interpret and to use. The different components of the wavefield, and the effects of different parts of the model on the wavefield, are more naturally separated in a ray solution than in a wave solution.

In this paper, I present a method for approximating the solution of a frequency-dependent version of the eikonal equation, also called "extended eikonal" by Zhu (1988), 'hypereikonal" by Beydoun (1985), and "exact' eikonal by Foreman (1989). The frequency dependent eikonal equation can be directly derived from the wave equation, via the Helmholtz equation, and does not rely on high-frequency assumptions. Its solution, together with the solution of the transport equation, provides an exact solution to the modeling problem. The numerical evaluation of the exact solution of the frequency-dependent eikonal is difficult, and thus I propose to compute an approximate solution. My method extrapolates in frequency the phase slowness by solving a non-linear partial differential equation. The extrapolation starts from infinite frequency, where the phase slowness is equal to the medium slowness, and moves down the frequency axis. Having computed the phase-slowness function, I solve the conventional eikonal using the computed phase-slowness function as the equivalent slowness of the medium. The method, although more expensive than simple raytracing, is still considerably cheaper than full-waveform modeling. It also retains many of the other attractive features of raytracing regarding the usability of the results. The direct application of my method for improving the accuracy of Kirchhoff migration should be straightforward, but it should also possible to apply it to seismic tomography.

In the first section I derive the frequency-dependent eikonal equation from the wave equation. In the second section I describe the slowness-extrapolation method for solving the "new" eikonal. Finally, in the third section I show the results of some preliminary numerical experiments using the proposed method, and compare the results with wave-equation modeling.

FREQUENCY-DEPENDENT EIKONAL

The frequency-dependent eikonal equation can be easily derived starting from the scalar wave equation:

$$\nabla^2 P\left(t, \vec{\mathbf{x}}\right) - S_0^2\left(\vec{\mathbf{x}}\right)\frac{\partial^2 P\left(t, \vec{\mathbf{x}}\right)}{\partial t^2} = 0, \tag{1}$$

where $P\left(t, \vec{\mathbf{x}}\right)$ is the wavefield, as a function of the position $\vec{\mathbf{x}}$ and time t, and $S_0\left(\vec{\mathbf{x}}\right)$ is the slowness of the medium. Fourier transforming the time coordinate we get the Helmholtz equation:

$$\nabla^2 \psi\left(\omega, \vec{\mathbf{x}}\right) + \omega^2 S_0^2\left(\vec{\mathbf{x}}\right)\psi\left(\omega, \vec{\mathbf{x}}\right) = 0, \tag{2}$$

where $\psi\left(\omega, \vec{\mathbf{x}}\right)$ is the transformed wavefield, and ω the temporal frequency.

The next step is to substitute into the Helmholtz equation the trial solution,

$$\psi\left(\omega, \vec{\mathbf{x}}\right) = A\left(\omega, \vec{\mathbf{x}}\right) e^{\imath\omega T\left(\omega, \vec{\mathbf{x}}\right)}, \tag{3}$$

where $A\left(\omega, \vec{\mathbf{x}}\right)$ is the amplitude of the wavefield, and $T\left(\omega, \vec{\mathbf{x}}\right)$ the time delay, or traveltime. Equating the real part of equation (2) we get the frequency-dependent eikonal equation, (Beydoun, 1985; Zhu, 1988)

$$S^2\left(\omega, \vec{\mathbf{x}}\right) = \left|\nabla T\left(\omega, \vec{\mathbf{x}}\right)\right|^2 = S_0^2\left(\vec{\mathbf{x}}\right) + \frac{1}{\omega^2}\frac{\nabla^2 A\left(\omega, \vec{\mathbf{x}}\right)}{A\left(\omega, \vec{\mathbf{x}}\right)}; \tag{4}$$

where $S^2\left(\omega, \vec{\mathbf{x}}\right)$ is the phase slowness, that is function of frequency. Equating the imaginary part of equation (2) we get the transport equation

$$\nabla \cdot \left[A^2\left(\omega, \vec{\mathbf{x}}\right)\nabla T\left(\omega, \vec{\mathbf{x}}\right)\right] = 0. \tag{5}$$

The conventional eikonal equation is derived by dropping the second term on the right of equation (4). The second term can be dropped when

$$\omega^2 \gg \frac{\nabla^2 A\left(\omega, \vec{\mathbf{x}}\right)}{A\left(\omega, \vec{\mathbf{x}}\right)}; \tag{6}$$

that is, when the frequency of the propagating waves is sufficiently large, with respect to the relative amplitude variations. In this case, the traveltimes are independent from the amplitudes, and the two equations can be solved sequentially. First, the eikonal is solved for the traveltimes; second, the amplitudes are computed using the transport equation. The most common method for computing the amplitudes is to recognize that the transport equation dictates that the product of the square of the amplitude with the phase slowness ($A^2 S$) is preserved along a ray tube. The amplitude can be thus expressed as

$$A\left(\omega, \vec{\mathbf{x}}\right) = A_0 S^{-\frac{1}{2}}\left(\omega, \vec{\mathbf{x}}\right) J^{-\frac{1}{2}}\left(\omega, \vec{\mathbf{x}}\right), \tag{7}$$

where A_0 is the amplitude at the source and $J(\omega, \vec{\mathbf{x}})$ is the Jacobian of mapping via rays (Bleistein, 1984). The amplitude is thus dependent on the phase slowness $S(\omega, \vec{\mathbf{x}})$, and on the Jacobian $J(\omega, \vec{\mathbf{x}})$, which is proportional to the ray density. The validity of the condition expressed in (6) is thus dependent on both the rate of variation of the phase slowness and on the rate of variation of ray density. For example, in presence of caustics, the condition in (6) can be violated even if the phase-slowness function is smooth.

SOLVING THE FREQUENCY-DEPENDENT EIKONAL

The frequency-dependent eikonal equation (4) cannot be solved separately from the transport equation because the phase slowness is dependent on the amplitudes. An exact numerical solution of the combined equations is difficult to compute. I therefore investigate a method for computing an approximate solution. My method extrapolates the phase-slowness function along the frequency axis, starting from infinite frequency where the phase slowness function is equal to the medium slowness. This scheme assumes that the phase slowness is a continuous function of frequency, and that it can be extrapolated in frequency by solving a partial differential equation. After the phase slowness function is computed, the traveltimes and the amplitudes can be computed at each frequency by using conventional dynamic raytracing (Červený, 1987).

To extrapolate the phase slowness I derive from equation (4) an expression for its derivative with respect to frequency. I start by rewriting equation (4) in terms of the inverse of the frequency $\phi = \frac{1}{\omega}$ and the square of the slowness $P(\phi) = S^2(\phi)$,

$$F(\phi, P) = P_0 - P(\phi) + \phi^2 \frac{\nabla^2 A[P(\phi), J(\phi)]}{A[P(\phi), J(\phi)]} = 0. \tag{8}$$

The derivative of $P(\phi)$ with respect to ϕ is found by applying the rule of implicit differentiation to the function $F(\phi, P)$

$$\frac{\partial P}{\partial \phi} = -\frac{\frac{\partial F(\phi,P)}{\partial \phi}}{\frac{\partial F(\phi,P)}{\partial P}} = \frac{2\phi \frac{\nabla^2 A[P(\phi),J(\phi)]}{A[P(\phi),J(\phi)]}}{1 - \phi^2 \frac{\partial}{\partial P} \left\{ \frac{\nabla^2 A[P(\phi),J(\phi)]}{A[P(\phi),J(\phi)]} \right\}}. \tag{9}$$

Equation (9) is a non-linear partial differential equation, that can be solved by explicitly stepping in ϕ, starting from the initial value $P(\phi = 0) = P_0$. For each value of ϕ, and corresponding value of $P(\phi)$, the right hand side of the equation can be evaluated and used for computing the value of the phase slowness for the next ϕ. A variety of explicit integration schemes can be used for integrating equation (9); I used a standard second-order Runge-Kutta method.

Because equation (9) is non-linear, the analysis of convergence and stability of its numerical solutions is not trivial, and I have not performed it yet. However, the numerical experiments that I have run, and that I will describe in the next section, show that the solution of equation (9) leads to satisfactory results. The solution is also stable, if the round-off errors for the high-wavenumbers components of the Laplacian of the phase slowness are adequately constrained.

Evaluation of derivatives of phase slowness with respect to frequency

The first quantity to be evaluated on the right hand side of equation (9) is the ratio between the Laplacian of the amplitude and amplitude itself. This term can be written as

$$
\begin{aligned}
L(\phi, P) &= \frac{\nabla^2 A\left[P(\phi), J(\phi)\right]}{A\left[P(\phi), J(\phi)\right]} \\
&= \left(A_0 P^{-\frac{1}{4}} J^{-\frac{1}{2}}\right)^{-1} A_0 \left[J^{-\frac{1}{2}} \nabla^2 \left(P^{-\frac{1}{4}}\right) + 2\nabla\left(P^{-\frac{1}{4}}\right)\nabla\left(J^{-\frac{1}{2}}\right) + P^{-\frac{1}{4}}\nabla^2\left(J^{-\frac{1}{2}}\right)\right] \\
&= P^{\frac{1}{4}}\nabla^2\left(P^{-\frac{1}{4}}\right) + 2P^{\frac{1}{4}} J^{\frac{1}{2}} \nabla\left(P^{-\frac{1}{4}}\right)\nabla\left(J^{-\frac{1}{2}}\right) + J^{\frac{1}{2}}\nabla^2\left(J^{-\frac{1}{2}}\right). \qquad (10)
\end{aligned}
$$

The second term to be evaluated is the derivative of $L(\phi, P)$ with respect to the phase slowness $P(\phi)$. In evaluating this term I neglect the dependency of the Jacobian $J(\phi)$ on the phase slowness, through the transport equation, because of the difficulties involved in computing the the derivatives of the Jacobian with respect to the phase slowness. Applying the chain rule to equation (10) I obtain:

$$
\begin{aligned}
&\frac{\partial}{\partial P}\left\{\frac{\nabla^2 A\left[P(\phi), J(\phi)\right]}{A\left[P(\phi), J(\phi)\right]}\right\} \\
&\quad = \left\{-A^{-2}[P, J]\frac{\partial A[P, J]}{\partial P}\nabla^2 A[P, J] + A^{-1}[P, J]\frac{\partial}{\partial P}\nabla^2 A[P, J]\right\} \\
&\quad = \left\{\frac{\nabla^2 A[P, J]}{4PA[P, J]} - \frac{J^{\frac{1}{2}}\nabla^2\left(J^{-\frac{1}{2}}\right)}{4P}\right\}. \qquad (11)
\end{aligned}
$$

The exact computation of either (10) or (11) requires the evaluation of the Jacobian at each frequency, and thus it requires performing full dynamic raytracing at each frequency. If results of raytracing were used the extrapolation should be repeated for every source position because the resulting phase-slowness function would be dependent on the source position. In contrast, when the terms dependent on the Jacobian are dropped, the same phase-slowness function can be used for all sources. Further, the Jacobian terms must be evaluated along all the branches of the wavefront. If bifurcations in the wavefront occur, the phase-slowness function would be multivalued. Implementing raytracing through such a function would be more cumbersome than through a single-valued slowness field. On the other hand, dropping the terms dependent on the Jacobian introduces errors where the rate of variations in ray density is large compared with the variations in phase slowness. For example, the accuracy of modeling waves propagating through caustic may be seriously affected.

For computing the results shown in the next section I used only the terms in equations (10) and (11) that are dependent on the phase slowness. As one could have expected, when the contributions of the Jacobian are neglected, the frequency extrapolation results in a progressive smoothing of the slowness function. This smoothing is consistent with the wave equation and, within the limitations in accuracy caused by the approximations that I have introduced, the "correct" amount of smoothing is applied at each frequency.

My raytracing routine does not compute amplitudes yet, thus I could not get a numerical estimate of the errors involved in neglecting the contribution of the Jacobian. However, I experimented with the analytical expression for the Jacobian valid in constant velocity; the inclusion of this "homogeneous" Jacobian had a very small effect on the resulting slowness. I expect that neglecting the contribution of the Jacobian will cause larger errors when the velocity inhomogeneities cause significant variations in ray density. As soon as I complete the implementation of dynamic raytracing on the Connection Machine, I will explore this issue more in depth.

The first term in equation (10) implies that the Laplacian operator is recursively applied to the phase-slowness function. Because the Laplacian operator amplifies the high-wavenumber components of the slowness, its recursive application may cause numerical instability. The high-wavenumber components of the round-off error may grow out of control. Instability can be avoided by applying a band-limited Laplacian. Only the round-off error should be attenuated when the Laplacian is filtered. The cut-off of the low-pass filter applied to the Laplacian must be above the maximum wavenumber present in the slowness function. I also noticed that decreasing the size of the extrapolation step resulted in a more stable solution.

MODELING RESULTS

To test the accuracy of the proposed solution of the frequency-dependent eikonal equation I compared results obtained by extrapolating the phase slowness with the results obtained from a wave-equation modeling by finite differences. I used two simple models for this testing. Both models present a Gaussian-shaped circular velocity anomaly in a constant velocity background, in the first example the perturbation is negative, in the second one it is positive. I chose anomalies of opposite signs because I wanted to test the accuracy of my method both in presence of focusing of the wavefield (negative perturbation) and of defocusing (positive perturbation).

In the first example the background velocity is 3 km/s, the maximum amplitude of the anomaly is 1.5 km/s and its width is about 100 m. I started the extrapolation process at infinite frequency and stopped when it reached the frequency of 5 Hz. The extrapolation step was constant in inverse frequency ϕ. Figure **??** shows a vertical slice of the resulting velocity model for three different frequencies. The solid line shows the medium slowness; that is, the infinite frequency slowness. The dashed line shows the phase slowness at 12.5 Hz, corresponding to a wavelength of 240 m. Finally the dotted line shows the phase slowness at 5 Hz, corresponding to a wavelength of 600 m. As frequency decreases, the frequency extrapolation progressively smooths the slowness model.

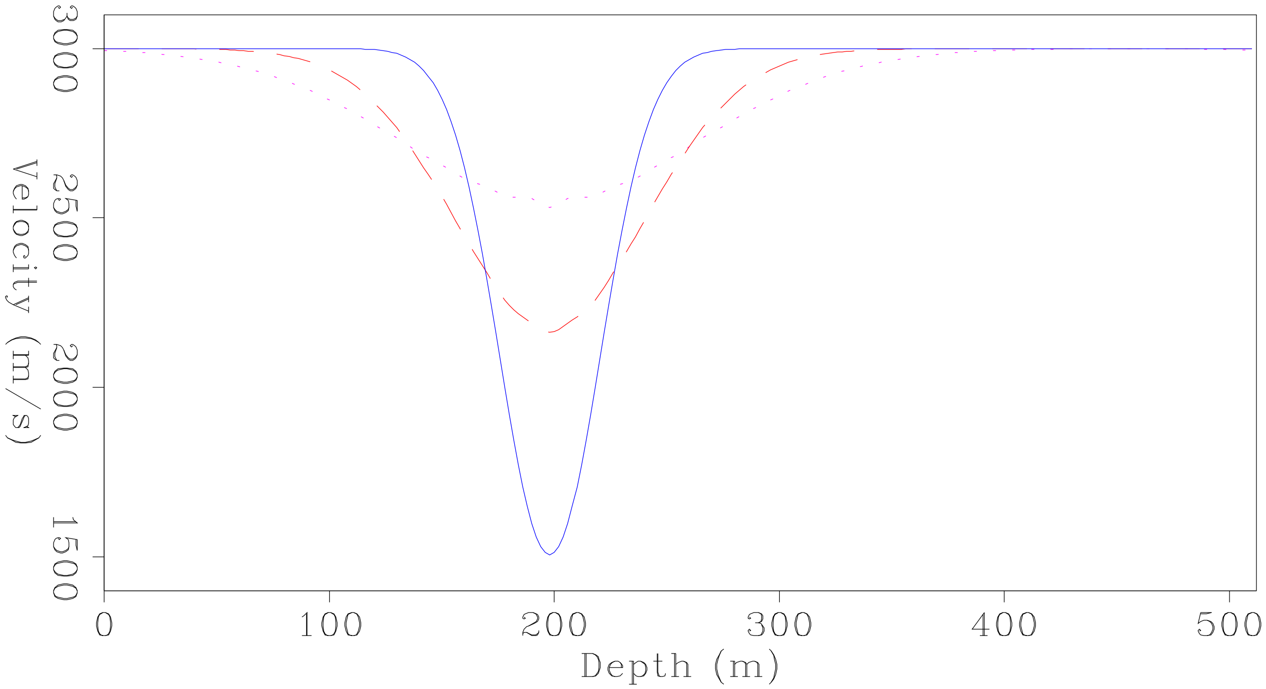

Figure 1: A vertical slice of the phase-slowness function for three different frequencies: infinite frequency (solid line), 12 Hz (dashed line), and 5 Hz (dotted line). biondo-Velneg [NR]

Figure **??** shows the results of wave-equation modeling and standard raytracing through the model. Plots of the rays (dashed lines) and the wavefront predicted by raytracing (solid black line) are superimposed onto a snapshot of the wavefield. The Figure also shows a contour plot of the velocity anomaly (white circles). For the wave-equation modeling I used a wavelet with central frequency of 60 Hz, corresponding to a wavelength of 50 m. This wavelength is sufficiently short, compared to the the width of the anomaly, for the eikonal to correctly predict the behavior of the wavefield. Just beneath the peak of the anomaly, the rays go through a caustic and the wavefront triplicates. The raytracing predicts correctly the positions and amplitudes of the different branches of the wavefield. In contrast, when the central frequency of the wavelet drops to 10 Hz (Figure **??**) the wavefront predicted by the eikonal does not match the actual wavefront of the wavefield. Figure **??** shows the result of wave-equation modeling with a 10 Hz wavelet and of raytracing through the extrapolated phase slowness at a frequency of 10 Hz. To facilitate the comparison, I actually plotted both the wavefront predicted by the phase slowness at 10 Hz (solid line) and the wavefront predicted by the medium slowness (dashed line). The low-frequency wavefront triplicates as well, but the inner branches are much shorter than the branches in the high-frequency wavefront. At the particular time of the snapshot, the low-frequency rays are still focused beneath the anomaly, consistently with the amplitudes of the actual wavefield, while the high frequency rays have already spread far apart.

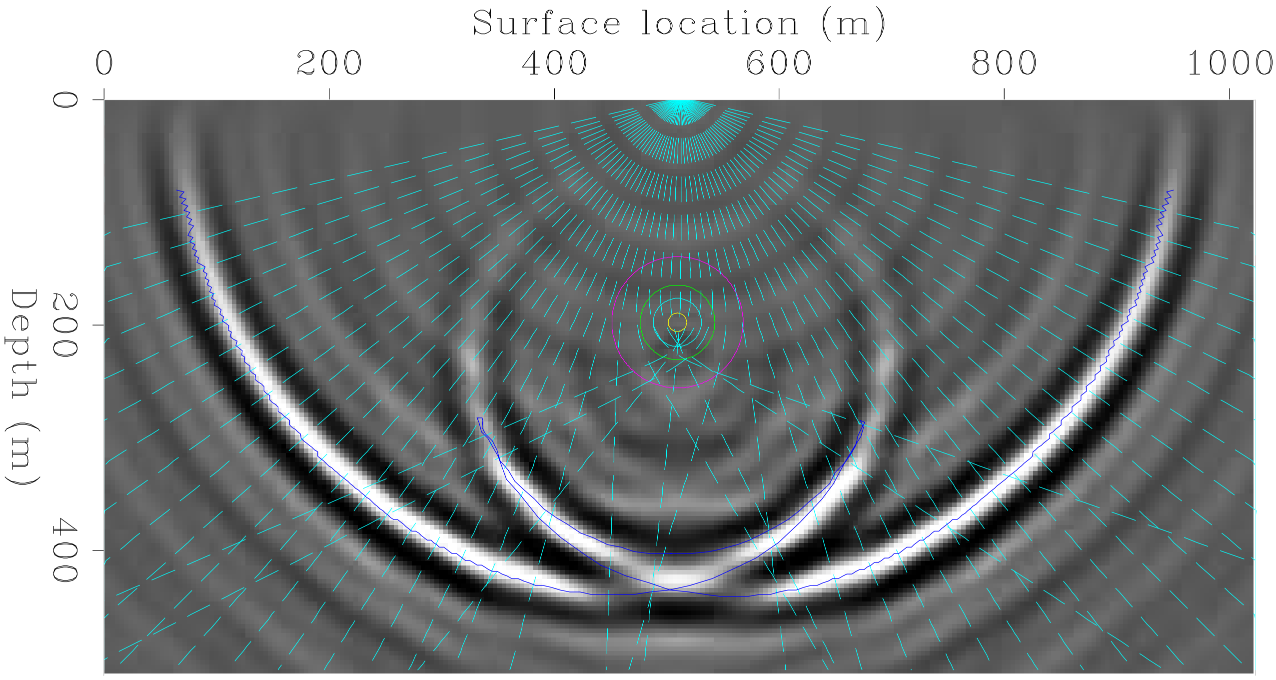

Figure 2: A snapshot of the wavefield generated by a source with central frequency of 60 Hz after propagating through the negative anomaly. Plots of the velocity anomaly, the rays traced through the medium slowness, and the wavefront predicted by the rays are superimposed onto the wavefield. biondo-Raynegvel60 [NR]

The second example is similar to the first, but the anomaly is positive instead of being negative, and thus the wavefield defocuses instead of focusing. The background velocity is 2 km/s, and the maximum amplitude of the anomaly is 1.5 km/s. I started the extrapolation process at infinite frequency, and stopped it when it reached 5 Hz. Figure **??** shows a vertical slice of the resulting velocity model for three different frequencies. The solid line in the Figure shows the medium slowness. The dashed line shows the phase slowness at 12.5 Hz, corresponding to a wavelength of 160 m. Finally the dotted line shows the phase slowness at 5 Hz, corresponding to a wavelength of 400 m. Also in this case the frequency extrapolation progressively smoothed the slowness function, but the respective scaling of the velocity perturbations are different from the previous example. In this case the 12.5 Hz anomaly has a peak of about 20% the peak of the infinite frequency slowness, when in the previous case it was about 50%. This behavior is a clear indication that the smoothing is far from being linear in velocity. Although, the smoothing might be close to be linear in slowness; this issue deserves further study.

Figure **??** shows the results of wave-equation modeling with a 60 Hz wavelet and of raytracing through the medium slowness. The rays (dashed lines) and the wavefront

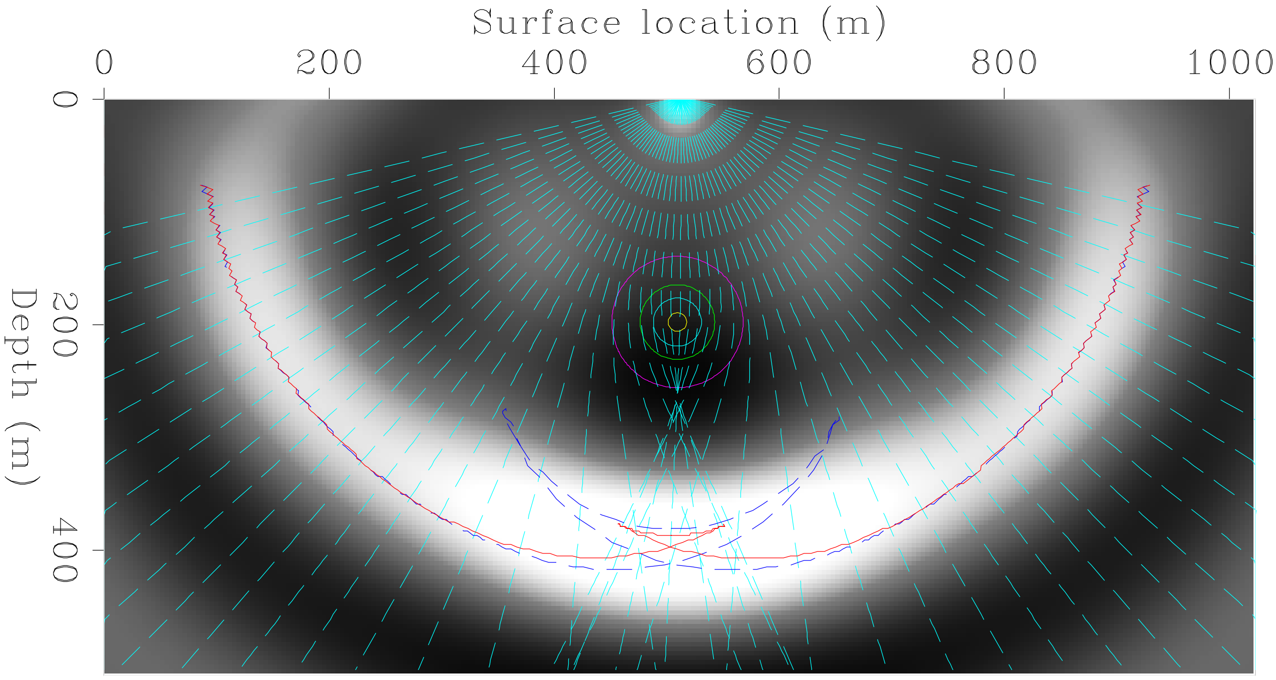

Figure 3: A snapshot of the wavefield generated by a source with central frequency of 10 Hz after propagating through the negative anomaly. Plots of the velocity anomaly, the rays traced through the 10 Hz phase slowness, and the wavefronts predicted by the 10 Hz phase slowness (solid line) and by the medium slowness (dashed line) are superimposed onto the wavefield. (Compare with Figure **??**) biondo-Raynegvel10 [NR]

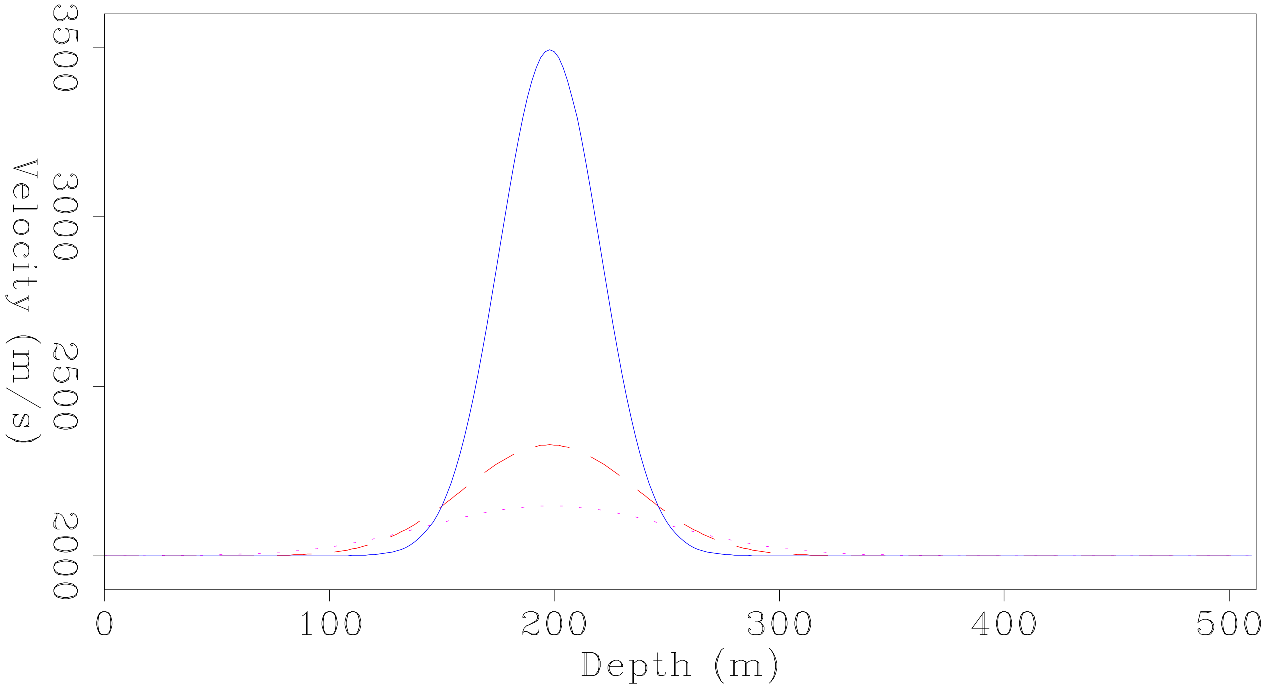

Figure 4: A vertical slice of the phase-slowness function for three different frequencies: infinite frequency (solid line), 12 Hz (dashed line), and 5 Hz (dotted line). (Compare with Figure **??**) biondo-Velpos [NR]

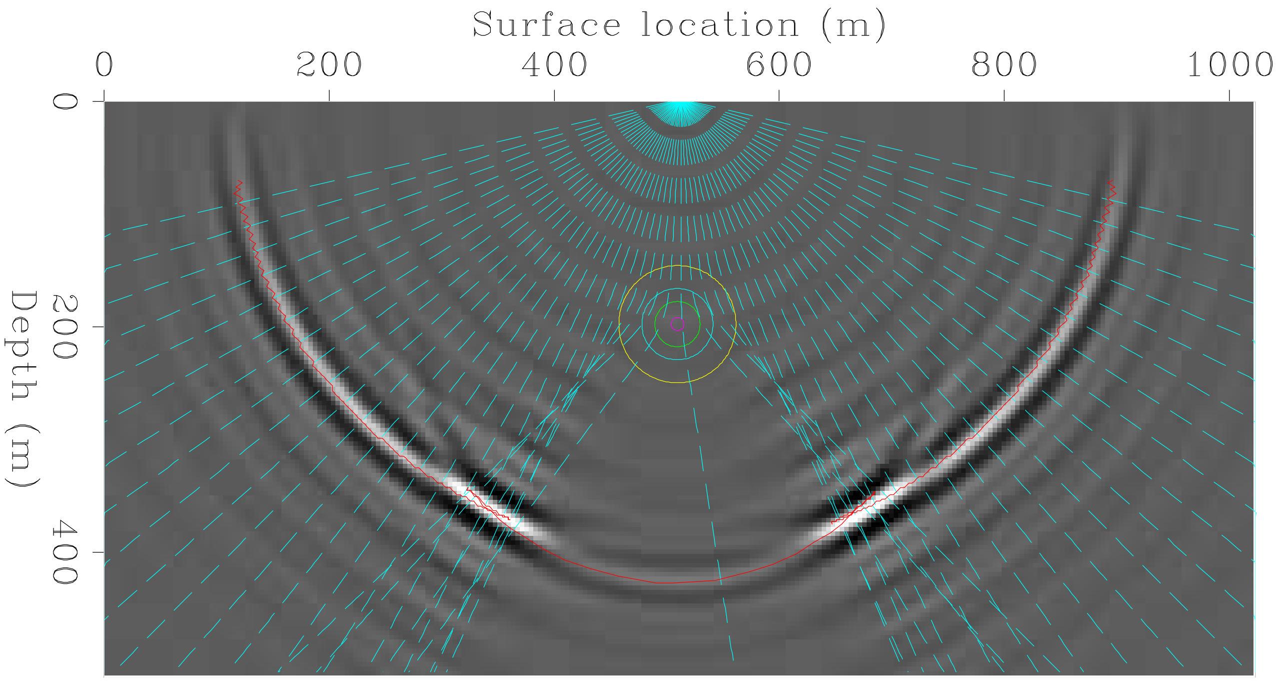

Figure 5: A snapshot of the wavefield generated by a source with central frequency of 60 Hz after propagating through the positive anomaly. Plots of the velocity anomaly, the rays traced through the medium slowness, and the wavefront predicted by the rays are superimposed onto the wavefield. biondo-Rayposvel60 [NR]

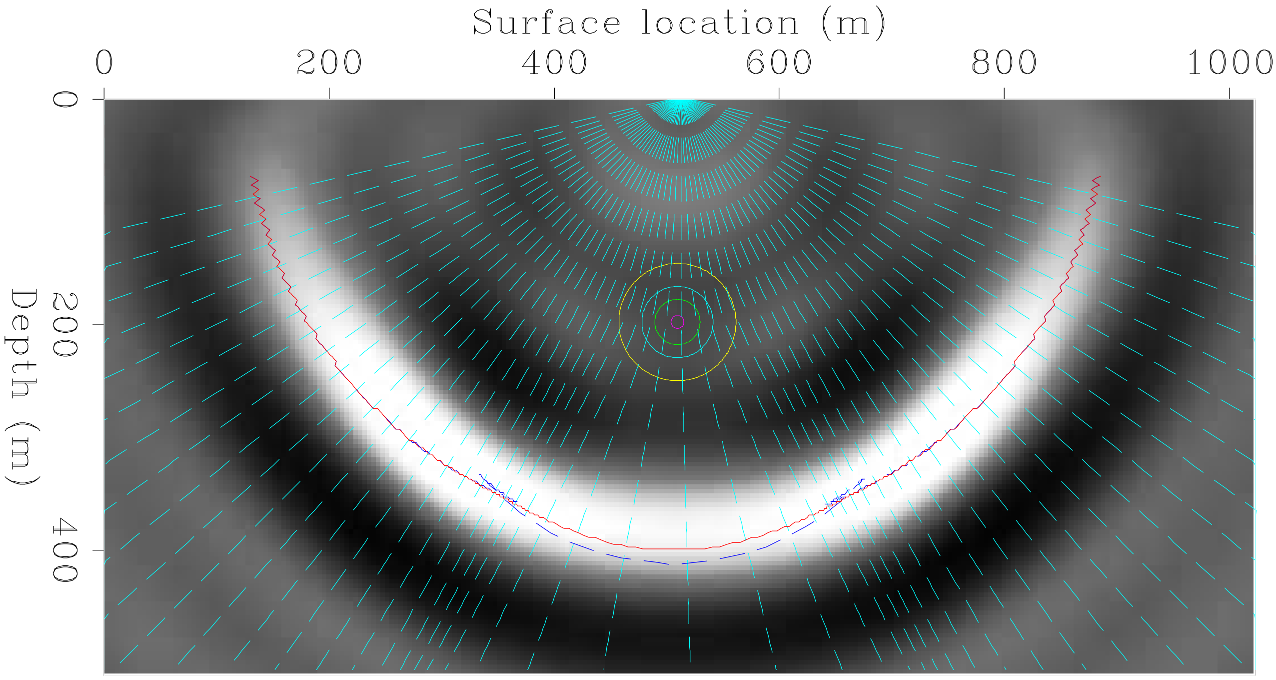

Figure 6: A snapshot of the wavefield generated by a source with central frequency of 10 Hz after propagating through the positive anomaly. Plots of the velocity anomaly, the rays traced through the 10 Hz phase slowness, and the wavefronts predicted by the 10 Hz phase slowness (solid line) and by the medium slowness (dashed line) are superimposed onto the wavefield. (Compare with Figure **??**) biondo-Rayposvel10 [NR]

predicted by raytracing (solid black line) are superimposed onto a snapshot of the wavefield. The wavefield is defocused by the anomaly; the anomaly causes a "shadow zone" beneath itself, where the amplitudes are very low. The high-frequency rays go through a caustic on either side of the anomaly, and thus the wavefront triplicates. The wavelength of the wavefield is too short (about 30 m) to observe wavefield dispersion and thus the raytracing through the medium slowness accurately predicts the behavior of the wavefield. In contrast, the low-frequency wavefield (Figure **??**) behaves quite differently from the high-frequency one. The wavefront does not triplicate and although the amplitudes beneath the anomaly are lower than on the side, they are not as low as in the high-frequency wavefield. The position of the wavefront and the amplitudes of the wavefield are well predicted by raytracing through the 10 Hz phase slowness computed using the frequency extrapolation method that I have presented. Beneath the anomaly, the distance between the wavefront predicted by the low-frequency phase slowness and the one predicted by the medium slowness is about 20 m; that is, the conventional eikonal would cause an error of about $\frac{\pi}{5}$ in modeling the propagation of a 10 Hz wavefield through the anomaly.

CONCLUSIONS

I have presented a method for solving the frequency-dependent eikonal equation by extrapolating the phase-slowness function along the frequency axis. When terms dependent on ray density are dropped from the extrapolation equation, the extrapolation turns out to be a frequency-dependent smoothing of the medium slowness. This smoothing is non linear, and it is consistent with the wave equation.

I tested the accuracy of the solution of the frequency-dependent eikonal both in presence of wavefield focusing and defocusing. In both cases the results of modeling using the proposed method match the result of modeling using the wave equation significantly better than the solution of the conventional eikonal equation.

Kirchhoff migration and seismic tomography are among the applications that I believe should gain from using my method of computing frequency-dependent traveltimes. But, more investigations are needed for determining the limitations and benefits of applying the new method to either problem.

REFERENCES

Beydoun, W. B., 1985, Asymptotic wave methods in heterogeneous media: Ph.D. thesis, MIT.

Bleistein, N., 1984, Mathematical methods for wave phenomena: Academic Press.

Červený, V., 1987, Ray tracing algorithms in three-dimensional laterally varying layered structures *in* Nolet, G., Ed., Seismic Tomography:: Riedel Publishing Co., 99–134.

Foreman, T. L., 1989, An exact ray theoretical formulation of the helmholtz equation: Journal of the Acoustical Society of America, **86**, 234–246.

Moser, T. J., 1989, Efficient seismic ray tracing using graph theory: 59th Annual Internat. Mtg., Soc. Expl. Geophys., Expanded Abstracts, 1106.

VanTrier, J., and Symes, W. W., 1991, Upwind finite-difference calculation of traveltimes: Geophysics, **56**, 812–821.

Vidale, J., 1988, Finite-difference calculation of travel times: Bull. Seism. Soc. Am., **78**, 2062–2076.

Woodward, M., 1990, Wave equation tomography: Ph.D. thesis, Stanford University.

Zhu, T., 1988, Ray-Kirchhoff migration in inhomogeneous media: Geophysics, **53**, 760–768.